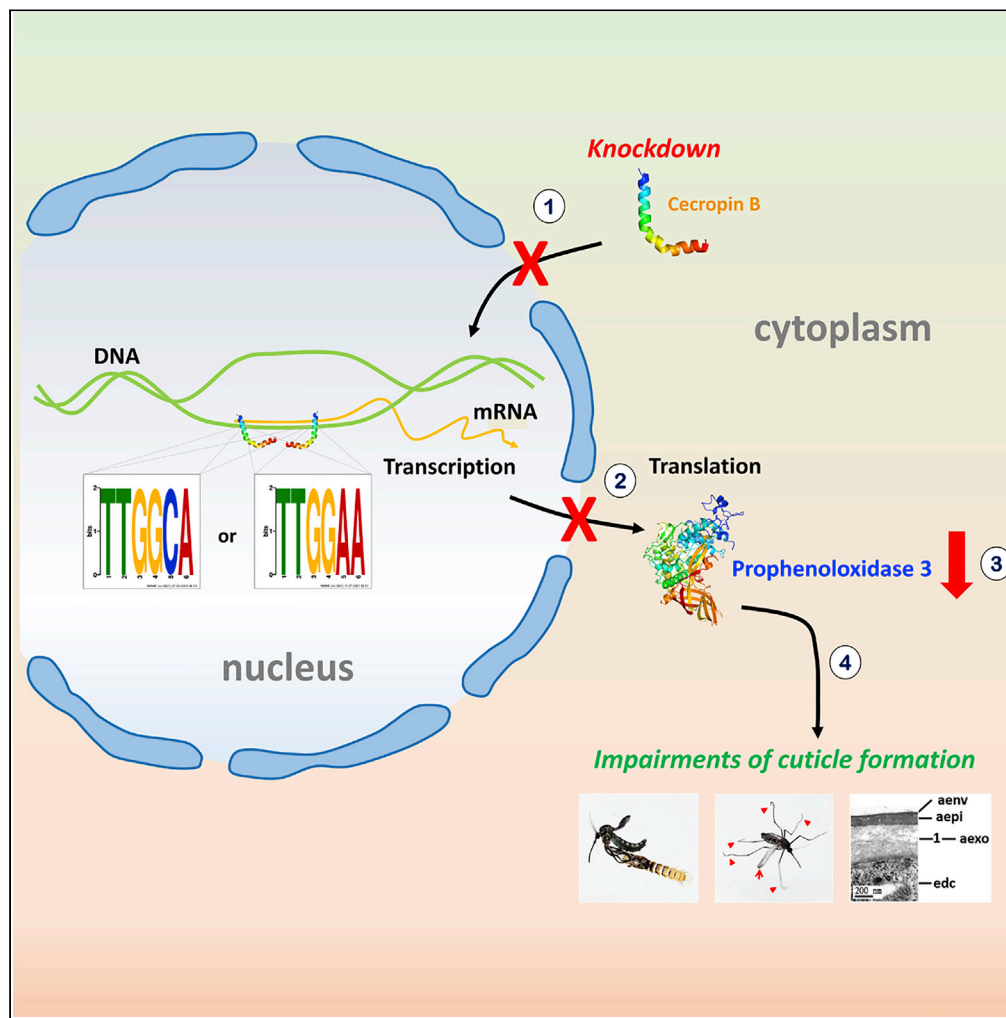# iScience

Article

The cecropin-prophenoloxidase regulatory mechanism is a cross-species physiological function in mosquitoes

Wei-Ting Liu,
Cheng-Chen
Chen, Dar-Der Ji,
Wu-Chun Tu

wctu@dragon.nchu.edu.tw

Highlights

Cecropin B is able to
regulate PPO 3 expression
in the pupae

Cecropin B binds to
TTGG(A/C)A motifs within
the PPO 3 DNA

The knockdown of
cecropin B was rescued by
sequence-similar cecropin
B peptides

The cecropin
B-prophenoloxidase 3
regulatory mechanism is
conserved in mosquitoes

CellPress
OPEN ACCESS

Article

The cecropin-prophenoloxidase regulatory mechanism is a cross-species physiological function in mosquitoes

Wei-Ting Liu,[1,2,6] Cheng-Chen Chen,[3] Dar-Der Ji,[3,4] and Wu-Chun Tu[5,7,*]

SUMMARY

This study's aim was to investigate whether the cecropin-prophenoloxidase regulatory mechanism is a cross-species physiological function among mosquitoes. BLAST and phylogenetic analysis revealed that three mosquito cecropin Bs, namely *Aedes albopictus* cecropin B (Aalcec B), *Armigeres subalbatus* cecropin B2 (Ascec B2), and *Culex quinquefasciatus* cecropin B1 (Cqcec B1), play crucial roles in cuticle formation during pupal development via the regulation of prophenoloxidase 3 (PPO 3). The effects of cecropin B knockdown were rescued in a cross-species manner by injecting synthetic cecropin B peptide into pupae. Further investigations showed that these three cecropin B peptides bind to TTGG(A/C)A motifs within each of the PPO 3 DNA fragments obtained from these three mosquitoes. These results suggest that Aalcec B, Ascec B2, and Cqcec B1 each play an important role as a transcription factor in cuticle formation and that similar cecropin-prophenoloxidase regulatory mechanisms exist in multiple mosquito species.

INTRODUCTION

Cuticle formation is an important event during pupal metamorphosis in insects. It is a complex process that starts with the detachment of the old cuticle from epidermal cells, which is followed by the formation of a new cuticle beneath the detached one (Costa et al., 2016); the next step involves sclerotization and melanization to stabilize the new exoskeleton. During the stabilization of the cuticular proteins, electrophilic quinones and quinone methides are generated by a phenoloxidase (PO) cascade and this leads to polymerization, with the quinones covalently cross-linking the cuticular structural proteins and the chitin (Suderman et al., 2006). This results in hardening of the cuticle. POs are multicopper tyrosinase-type phenol oxidases and have long been suggested to play critical roles in many physiological functions of insects, including cuticular sclerotization, cuticle formation, egg tanning, wound healing, and the melanotic encapsulation of pathogens (Locke and Krishnan, 1971; Cho et al., 1998; Huang et al., 2001; Shiao et al., 2001; Marinotti et al., 2014; Tsao et al., 2015; Liu et al., 2017). POs are present in a zymogen form in insects, namely as prophenoloxidases (PPOs). Tsao et al. (2010) demonstrated that *Armigeres subalbatus* prophenoloxidase III (As-pro-PO III) is required for cuticle formation in *Ar. subalbatus* pupae.

Recently, Liu et al. (2017) found a mosquito antimicrobial peptide (AMP), *Aedes aegypti* cecropin B (Aacec B), plays a crucial role in pharate adult cuticle formation via the regulation of *Ae. aegypti* prophenoloxidase 3 (AaPPO 3). Aacec B seems to act as a transcription factor that is able to regulate AaPPO 3 expression in pupae. Hence, this study aimed to elucidate whether the cecropin-prophenoloxidase regulatory mechanism also functions in the other species of mosquitoes. The results of the present study demonstrate that the amino acid sequences of three mosquito cecropin B, namely *Aedes albopictus* cecropin B (Aalcec B), *Armigeres subalbatus* cecropin B2 (Ascec B2), and *Culex quinquefasciatus* cecropin B1 (Cqcec B1), are highly similar to that of Aacec B, and play a significant and similar role to Aacec B whereby they modulate PPO 3 gene transcription in *Ae. albopictus*, *Ar. subalbatus*, and *Cx. quinquefasciatus*; this occurs through binding to TTGG(A/C)A DNA motifs during pupal metamorphosis.

RESULTS

The amino acid sequences of cecropin B from *Aedes albopictus*, *Armigeres subalbatus*, and *Culex quinquefasciatus* are highly similar to that of *Aedes aegypti* cecropin B

To investigate whether the cecropin-prophenoloxidase regulatory mechanism is conserved in insects, a BLAST analysis was conducted to search for homologous sequences using the amino acid sequence of

[1]Institute of Microbiology and Immunology, National Yang Ming Chiao Tung University, Taipei 112, Taiwan

[2]Institute of Molecular Biology, Academia Sinica, Taipei 115, Taiwan

[3]Department of Tropical Medicine, National Yang Ming Chiao Tung University, Taipei 112, Taiwan

[4]One Health Research Center, National Yang Ming Chiao Tung University, Taipei 112, Taiwan

[5]Department of Entomology, National Chung Hsing University, Taichung 402, Taiwan

[6]Present address: Department of Entomology, National Chung Hsing University, Taichung 402, Taiwan

[7]Lead contact

*Correspondence: wctu@dragon.nchu.edu.tw

https://doi.org/10.1016/j.isci.2022.104478

Figure 1. Phylogenetic analysis and amino acid sequence alignment of various cecropin peptides

(A) Neighbor-Joining distance phylogenetic tree showing the relationship between various cecropins and various cecropin-like peptides. The amino acid sequences of 112 cecropins from Diptera [*Ae. aegypti* (n = 10); *Ae. albopictus* (n = 7); *An. albimanus* (n = 3); *An. arabiensis* (n = 2); *An. gambiae* (n = 4); *An. minimus* (n = 4); *An. quadriannulatus* (n = 1); *An. sinensis* (n = 2); *An. stephensi* (n = 4); *Ar. subalbatus* (n = 5); *Cx. quinquefasciatus* (n = 5); *Drosophila mauritiana* (n = 6), *Drosophila melanogaster* (n = 4); *Drosophila pseudoobscura* (n = 3); *Malus domestica* (n = 4); *Stomoxys calcitrans* (n = 2)], Lepidoptera [*Bombyx mori* (n = 5); *Helicoverpa armigera* (n = 4); *Hyalophora cecropia* (n = 3); *Hyphantria cunea* (n = 1); *Manduca sexta* (n = 1); *Operophtera brumata* (n = 2); *Ostrinia furnacalis* (n = 1); *Papilio machaon* (n = 1); *Papilio xuthus* (n = 3); *Plutella xylostella* (n = 4); *Spodoptera exigua* (n = 6); *Trichoplusia ni* (n = 3)],

Figure 1. *Continued*

Coleoptera [*Acalolepta luxuriosa* (n = 1); *Calomera littoralis* (n = 2); *Diabrotica virgifera virgifera* (n = 2)], Nematoda [*Ascaris suum* (n = 4)] and tunicates [*Styela clava* (n = 3)] were selected for the tree construction. The mosquito cecropins are shown in green, the four target mosquito species are shown in red, and other dipteran species are shown in light blue, while the coleopteran is shown in purple, the nematodes are shown in black, the tunicates are shown in blue, and the lepidopterans are shown in orange.

(B) Alignment of cecropin B proteins of *Aedes aegypti*, *Aedes albopictus*, *Armigeres subalbatus*, and *Culex quinquefasciatus*. All sequences were obtained from NCBI protein database and VectorBase database. Symbol (*) indicates that the aligned residues are identical. Substitutions suggested to be conservative or semi-conservative are marked as (:) and (.), respectively.

Ae. aegypti cecropin B (Aacec B); the search included 83 insect species, namely five species belonged to Coleoptera, sixteen to Diptera, twelve to Hemiptera, thirty-eight to Hymenoptera, and twelve to order Lepidoptera. A total of 105 cecropins from 31 insect species, belonging to Coleoptera, Diptera, and Lepidoptera, were identified as homologs of Aacec B; however, no homologs of Aacec B were found among hymenopteran and hemipteran insects. Further phylogenetic analysis of these 105 cecropin was carried out using four nematode cecropins and three tunicate cecropin-like peptides as outgroups and this showed that the cecropin sequences could be divided into five distinct clusters (Figure 1A). In cluster V, three cecropins, *Ae. albopictus* cecropin B (VectorBase: AALF014650), *Ar. subalbatus* cecropin B2 (GenBank: AY440667.1), and *Cx. quinquefasciatus* cecropin B1 (VectorBase: CPIJ005108) cluster with Aacec B and are distinct from other insect cecropins. Sequence alignment analysis showed that the deduced amino acid sequences of the three Aacec B homologs, namely *Ae. albopictus* cecropin B (Aalcec B), *Ar. subalbatus* cecropin B2 (Ascec B2), and *Cx. quinquefasciatus* cecropin B1 (Cqcec B1), are highly similar (identity >92% and similarity >94%) to the sequence of Aacec B (Figure 1B and Table S2).

Knockdown of cecropin B in the pupae of *Ae. albopictus*, *Ar. subalbatus*, and *Cx. quinquefasciatus* leads to a high pupal mortality and the emergence of deformed adults; these deleterious effects of cecropin B knockdown are rescued in a cross-species manner

In order to investigate whether the three cecropin Bs have similar physiological functions compared to Aacec B, we examined the expression levels and the effects of knockdown of Aalcec B, Ascec B2, and Cqcec B1 on *Ae. albopictus*, *Ar. subalbatus*, and *Cx. quinquefasciatus*, respectively. At 26 ± 1°C, the lengths of the pupal stage of *Ae. albopictus*, *Ar. subalbatus*, and *Cx. quinquefasciatus* are approximately 52.1, 79.8, and 50.5 h, respectively. Thus, the effect of knockdown of Aalcec B and Cqcec B1 in *Ae. albopictus* and *Cx. quinquefasciatus*, respectively, was recorded at 48 h after larval-pupal ecdysis, while that of Ascec B2 in *Ar. subalbatus* was recorded at 72 h after larval-pupal ecdysis. As shown in Figures 2A–2C, the mRNA levels of Aalcec B, Ascec B2, and Cqcec B1 were detectable at < 0.5 h after ecdysis, that is immediately after larval-pupal ecdysis, and then decreased to low levels at 12–36 h. Later, these mRNA were highly expressed in *Ar. subalbatus* at 72 h after ecdysis (Figure 2B) and in *Cx. quinquefasciatus* at 48 h after ecdysis (Figure 2C). However, the expression level of Aalcec B in *Ae. albopictus* was only slightly increased at 48 h after ecdysis (Figure 2A). Compared with the uninjected and the GFP dsRNA-injected mosquitoes, the mRNA levels of cecropin B were found to be significantly reduced in the three mosquito species after cecropin B dsRNA was injected into the pupae.

Injection of cecropin B dsRNA into mosquito pupae resulted in a high level of pupal mortality. As shown in Figure 2D, the cumulative mortality rate was 63.13 ± 5.94% after the pupae of *Ae. albopictus* was injected with Aalcec B dsRNA alone. The mortality rate was reduced to 27.22 ± 3.28% after injection simultaneously with Aalcec B dsRNA and Aacec B peptide, 25 ± 11.89% after injection simultaneously with Aalcec B dsRNA and Aalcec B peptide, 27.78 ± 6.21% after injection simultaneously with Aalcec B dsRNA and Ascec B2 peptide, and 26 ± 12.84% after injection simultaneously with Aalcec B dsRNA and Cqcec B1 peptide. Similar reductions in cumulative mortality were also observed in *Ar. subalbatus* and *Cx. quinquefasciatus*. As shown in Figure 2E, the cumulative mortality rate was 70.95 ± 11.34% in Ascec B2 dsRNA-injected pupae of *Ar. subalbatus*, which was reduced to 31.67 ± 5.48% after injection simultaneously with Ascec B2 dsRNA and Aacec B peptide, 32.67 ± 18.65% after injection simultaneously with Ascec B2 dsRNA and Aalcec B peptide, 32.22 ± 9.35% after injection simultaneously with Ascec B2 dsRNA and Ascec B2 peptide, and 36.67 ± 12.07% after injection simultaneously with Ascec B2 dsRNA and Cqcec B1 peptides. The cumulative mortality rate was 61.67 ± 9.76% in Cqcec B1 dsRNA-injected pupae of *Cx. quinquefasciatus*, which was reduced to 28.89 ± 4.04% after injection simultaneously with Cqcec B1 dsRNA and Aacec B peptide, 27.33 ± 4.66% after injection simultaneously with Cqcec B1 dsRNA and Aalcec B peptide, 26.67 ± 5.58% after injection simultaneously with Cqcec B1 dsRNA and Ascec B2 peptide, and 27 ± 7.93% after injection simultaneously with Cqcec B1 dsRNA and Cqcec B1 peptide (Figure 2F). However, a reduction in mortality rate was not observed in pupae injected simultaneously with cecropin B dsRNA and
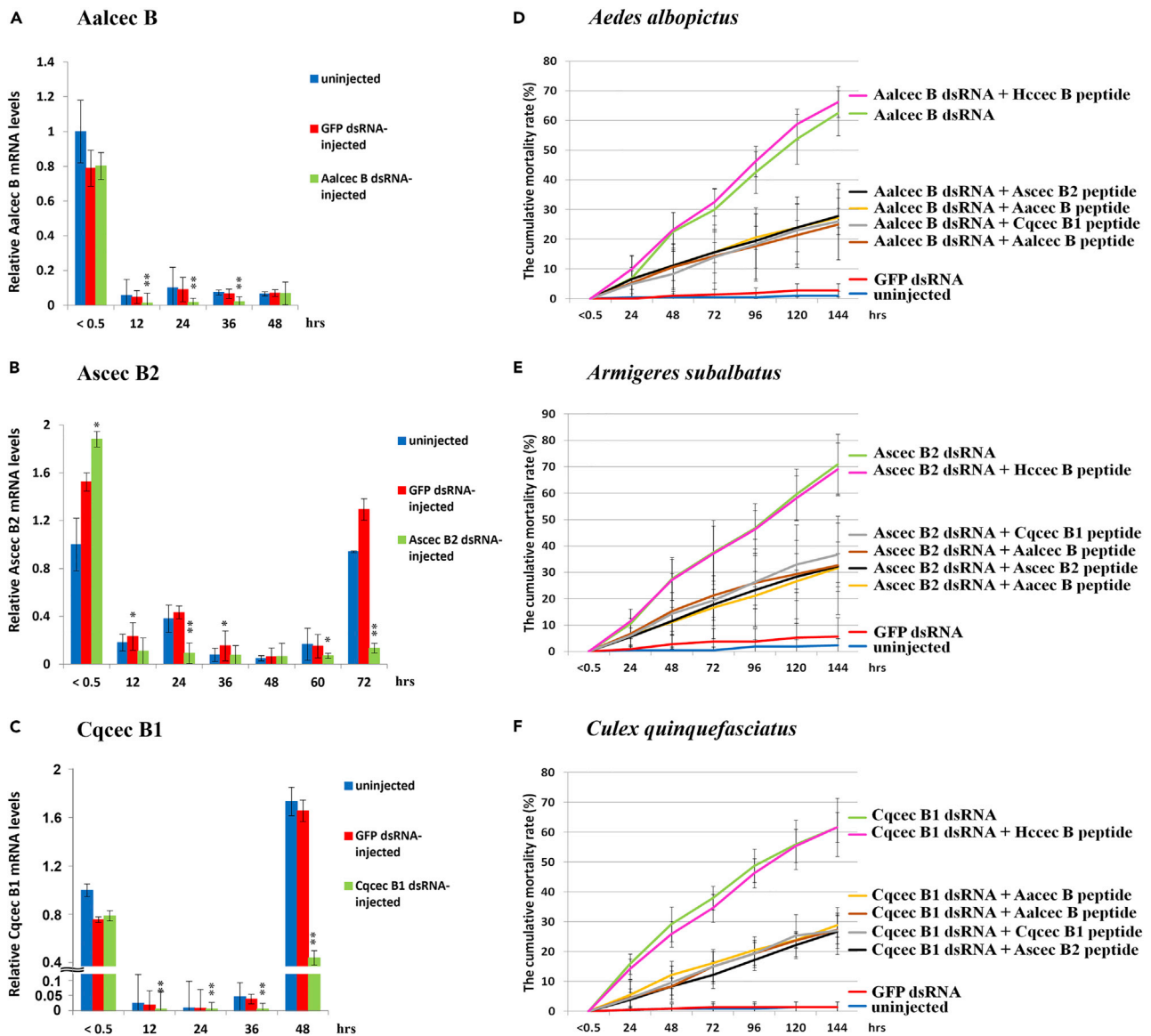
Figure 2. The effects of gene knockdown on cecropin B expression in pupae of *Aedes albopictus*, *Armigeres subalbatus*, and *Culex quinquefasciatus*

(A–C) RT-qPCR analysis of cecropin B expression in the uninjected control, the GFP dsRNA-injected control, and the cecropin B dsRNA-injected pupae. 0.5–72: <0.5–72 h after injection. qPCR results were normalized against the mRNA expression of *Ae. albopictus* ribosomal protein L32 (AalRPL32), *Ar. subalbatus* ribosomal protein S7 (AsS7), and *Cx. quinquefasciatus* ribosomal protein S7 (CqS7), respectively. Values are means ± SD, n = 3. Asterisks indicate significant differences (*$p < 0.005$; **$p < 0.001$) compared to the relative mRNA levels of the uninjected control at each time point. (A) *Ae. albopictus* cecropin B (Aalcec B). (B) *Ar. subalbatus* cecropin B2 (Ascec B2). (C) *Cx. quinquefasciatus* cecropin B1 (Cqcec B1).

(D–F) The cumulative mortality rates (%) of the uninjected control (blue line), the GFP dsRNA-injected control (red line), the cecropin B dsRNA-injected pupae (green line), the cecropin B dsRNA + Aacec B peptide-injected pupae (orange line), the cecropin B dsRNA + Aalcec B peptide-injected pupae (brown line), the cecropin B dsRNA + Ascec B2 peptide-injected pupae (black line), the cecropin B dsRNA + Cqcec B1 peptide-injected pupae (gray line), and the cecropin B dsRNA + *Hyalophora cecropia* cecropin B (Hccec B) peptide-injected pupae (pink line) at various time intervals after injection. < 0.5–144: <0.5–144 h after injection. Each group consisted of thirty pupae in a single experiment and seven replicate experiments were conducted. The range bars indicates the standard deviations of the means. (D) *Ae. albopictus*. (E) *Ar. subalbatus*. (F) *Cx. quinquefasciatus*.

Hyalophora cecropia cecropin B (Hccec B) peptide (Figures 2D–2F). Among the above pupae, 1.79% of the Aalcec B dsRNA-injected pupae, 3.17% of the Ascec B2 dsRNA-injected pupae, and 1.11% of the Cqcec B1 dsRNA-injected pupae emerged as deformed adults with curved legs or wings and then died shortly after emergence. Only two *Ae. albopictus* injected simultaneously with Aalcec B dsRNA and Aacec B peptide,

one *Ar. subalbatus* injected simultaneously with Ascec B2 dsRNA and Cqcec B1 peptide, and one *Cx. quinquefasciatus* injected simultaneously with Cqcec B1 dsRNA and Aalcec B peptide emerged as deformed adults. These findings support the hypothesis that each of the peptides, Aalcec B, Ascec B2, and Cqcec B1, plays as an important role as Aacec B in pupal morphogenesis. Furthermore, the knockdown effects of cecropin B were rescued in a cross-species manner in all three cases by the injection of a sequence-similar cecropin B peptide from different mosquito species.

Knockdown of cecropin B in pupae leads to a reduction in the transcription of PPO 3 in *Ae. albopictus*, *Ar. subalbatus*, and *Cx. quinquefasciatus*

To elucidate whether the effects of knockdown of the three cecropin Bs also affect gene expression of their respective prophenoloxidase 3s during pupal development, we examined the expression levels of prophenoloxidase 3 (PPO 3) after the pupae was injected with cecropin B dsRNA alone. A BLAST analysis was first conducted to search for homologs of the amino acid sequence of AaPPO 3 in *Ae. albopictus*, *Ar. subalbatus*, and *Cx. quinquefasciatus*. As shown in Figure 3, AaPPO 3 clustered together with three prophenoloxidase genes, namely *Ae. albopictus* prophenoloxidase 3 (AalPPO 3) (AALF011778), *Ar. subalbatus* prophenoloxidase 3 (As-pro-PO III) (AAR88078.1), and *Cx. quinquefasciatus* prophenoloxidase 3 (CqPPO 3) (CPIJ009877), and these had high degrees of amino acid sequence similarity to AaPPO 3 (Figure S1 and Table S3). As shown in Figures 4A and 4C, the mRNA levels of AalPPO 3 and CqPPO 3 were detectable at < 0.5 h after ecdysis immediately after larval-pupal ecdysis, and were expressed constitutively over the time period 12–48 h after ecdysis. The mRNA levels were highly expressed in *Ae. albopictus* and *Cx. quinquefasciatus* at 24 h after ecdysis. While the mRNA of As-pro-PO III was detectable at < 0.5 h after ecdysis immediately after larval-pupal ecdysis, it then decreased to a low level, and this was then followed by constitutive expression at 12–72 h after ecdysis. In addition, the expression level of As-pro-PO III was found to be slightly increased at 60 h after ecdysis in *Ar. subalbatus* (Figure 4B).

Subsequently, we investigated the knockdown effects of cecropin B on the transcription of PPO 3 in *Ae. albopictus*, *Ar. subalbatus*, and *Cx. quinquefasciatus*. When compared with uninjected mosquitoes, knockdown of Aalcec B significantly reduced the transient expression of AalPPO 3 in *Ae. albopictus* at 12–48 h after ecdysis (Figure 4A). Furthermore, knockdown of Ascec B2 significantly reduced transient expression of As-pro-PO III in *Ar. subalbatus* at 36, 60, and 72 h after ecdysis (Figure 4B). Finally, knockdown of Cqcec B1 significantly reduced transient expression of CqPPO 3 in *Cx. quinquefasciatus* at 12–36 h after ecdysis (Figure 4C). Furthermore, knockdown of Cqcec B1 also significantly induced the expression levels of CqPPO 3 in *Cx. quinquefasciatus* at 48 h after larval-pupal ecdysis (Figure 4C). This implies that the CqPPO 3 dsRNA injection might be not sufficient to suppress the transcription of CqPPO 3 for 48 h, which, in turn, activates the expression of CqPPO 3. These findings indicate that knockdown of cecropin B decreased the transcription levels of PPO 3 in pupae of *Ae. albopictus*, *Ar. subalbatus*, and *Cx. quinquefasciatus*.

Cuticle formation is impaired in the cecropin B-knockdown pupae of *Ae. albopictus*, *Ar. subalbatus*, and *Cx. quinquefasciatus*

Cuticle formation is one of the major morphogenetic events during the pupal stage. Since there was high mortality and only a few deformed adults available after cecropin B dsRNA injection, we used transmission electron microscopy to study the cuticular ultrastructure of the cecropin B-knockdown pupae of the three species. The time point used for ultrastructural observations in *Ae. albopictus* and *Cx. quinquefasciatus* was 48 h after larval-pupal ecdysis, while that used for *Ar. subalbatus* was 72 h after larval-pupal ecdysis. As shown in Figure 5A, the cuticles of the uninjected *Ae. albopictus* pupae consist of a pupal and a pharate adult cuticle. The pupal cuticle consisted of an envelope, an epicuticle, a seven-laminated exocuticle, and a fifteen-laminated endocuticle. The pharate adult cuticle consisted of an envelope, an epicuticle, and one six-laminated exocuticle. The chitin microfibrils within the chitin-protein matrix in the fully formed exocuticle lamellae of the pharate adult cuticle are arranged in an electron-dense helicoidal pattern. However, although the ultrastructure of the pupal cuticle of the Aalcec B dsRNA-injected mosquitoes remains similar to that of the GFP dsRNA-injected and uninjected pupae, cuticle formation by the pharate adult of Aalcec B dsRNA-injected pupae was significantly impaired. For example, only one-laminated exocuticle of the pharate adult cuticle was deposited by the Aalcec B dsRNA-injected pupae, and the helicoidal pattern of the chitin microfibrils was disorganized; furthermore, there were numerous irregular electron-lucent spaces present within the chitin-protein matrix. Notwithstanding the above, injection of Aalcec B peptide seems to rescue the effects of Aalcec B knockdown; specifically, there was a three-laminated exocuticle of the pharate adult cuticle deposited in pupae injected simultaneously with Aalcec B dsRNA and Aalcec B peptide.
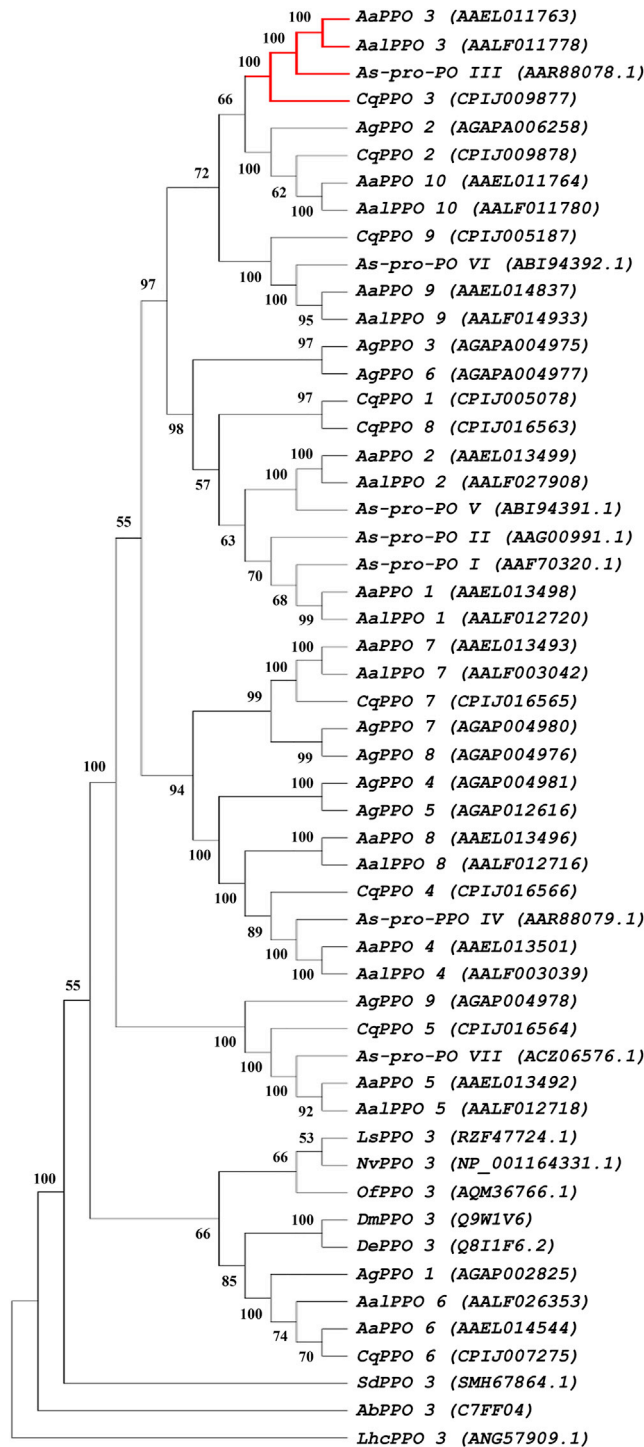
Figure 3. Phylogenetic analysis of various prophenoloxidase (PPO) peptides

Neighbor-Joining distance phylogenetic tree showing the relationship between the PPOs. The amino acid sequences of fifty PPOs from genomic databases were used for tree construction; these were from ten insect species, including seven species belonged to Diptera [*Ae. aegypti* (n = 10); *Ae. albopictus* (n = 10); *An. gambiae* (n = 9); *Ar. subalbatus* (n = 7); *Cx. quinquefasciatus* (n = 9), *Drosophila erecta* (n = 1), *Drosophila melanogaster* (n = 1)], one to Hemiptera [*Laodelphax striatellus* (n = 1)], one to Hymenoptera [*Nasonia vitripennis* (n = 1)], and one to Lepidoptera [*Ostrinia furnacalis* (n = 1)]. The amino acid sequences of prophenoloxidase 3 (PPO 3) from a Chilopoda [*Scolopendra dehaani* (n = 1)], a fungus [*Agaricus bisporus* (n = 1)], and a lilium [*Lilium* hybrid cultivar (n = 1)] were used as outgroups.
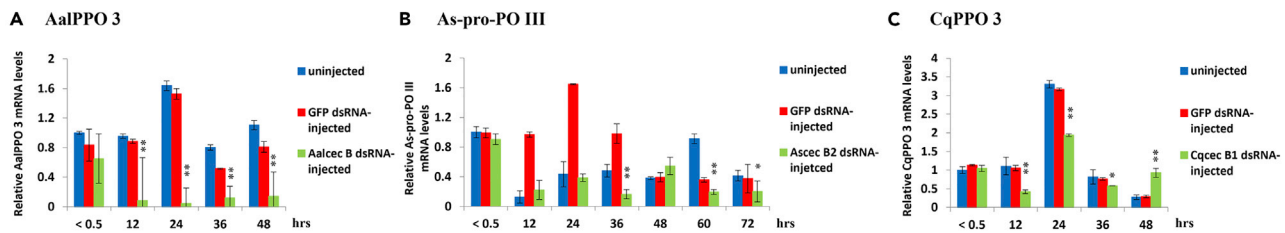
Figure 4. RT-qPCR analysis of prophenoloxidase 3 expression levels in uninjected control, GFP dsRNA-injected control, and cecropin B dsRNA-injected pupae of mosquitoes

(A) *Aedes albopictus*, (B) *Armigeres subalbatus*, and (C) *Culex quinquefasciatus*. 0.5–72: <0.5–72 h after injection. The qPCR results are normalized against the mRNA expression level of *Ae. albopictus* ribosomal protein L32 (AalRPL32), *Ar. subalbatus* ribosomal protein S7 (AsS7), and *Cx. quinquefasciatus* ribosomal protein S7 (CqS7), respectively. Values are means ± SD, n = 3. Asterisks indicate significant differences (*$p < 0.005$; **$p < 0.001$) compared to the appropriate mRNA levels of the uninjected control at each time point. (A) *Ae. albopictus* prophenoloxidase 3 (AalPPO 3).
(B) *Ar. subalbatus* prophenoloxidase III (As-pro-PO III). (C) *Cx. quinquefasciatus* prophenoloxidase 3 (CqPPO 3).

However, the helicoidal pattern of the chitin microfibrils of pupae injected simultaneously with Aalcec B dsRNA and Aalcec B peptide seems not to be as neat as those of the uninjected pupae of *Ae. albopictus*.

Similar effects were also observed when the ultrastructures of pupal and pharate adult cuticles of *Ar. subalbatus* and *Cx. quinquefasciatus* were investigated. As shown in Figures 5B and 5C, knockdown of cecropin B resulted in only one laminated exocuticle of pharate adult cuticle being deposited by *Ar. subalbatus* and *Cx. quinquefasciatus*. The helicoidal patterns of the chitin microfibrils were also disorganized with numerous irregular electron-lucent spaces being present in both species. This could be contrasted in *Ar. subalbatus* and *Cx. quinquefasciatus* with the three-laminated exocuticle of the pharate adult cuticle that was present in pupae that had been injected simultaneously with cecropin B dsRNA and cecropin B peptide. In addition, the chitin microfibrils of these insect were organized almost as neatly as the helicoidal structures of the uninjected mosquito of *Ar. subalbatus* and *Cx. quinquefasciatus*.

Cecropin B is detectable in the cell nuclei of pupae of *Ae. albopictus*, *Ar. subalbatus*, and *Cx. quinquefasciatus*

Based on the above, the three cecropin Bs might be able to be translocated into nucleus and then bind to specific DNA motifs in order to regulate the expression of their respective PPO 3 genes. We used Western blotting to detect the presence of cecropin B in the pupal cells of *Ae. albopictus*, *Ar. subalbatus*, and *Cx. quinquefasciatus*. As shown in Figures 6A-1, 6B-1, 6C-1, and S2, Ascec B2 antibody was able to detect a single band of synthetic cecropin B peptide that has an estimated molecular weight of approximately 4 kDa (the theoretical molecular weight of synthetic Ascec B2 is 3.75 kDa, Aalcec B is 3.76 kDa, and Cqcec B1 is 3.79 kDa). The same antibody was also able to detect two bands in a total protein extract from pupae. The molecular weights of these two bands were approximately 11 and 34 kDa, which correspond to trimers and nonamers of Ascec B2, respectively (Figure 6B-1). Subsequently, we examined the presence of cecropin B in both the cytoplasm and nucleus of pupal cells. As shown in Figures 6B-2 and 6B-3, the trimer and nonamer of Ascec B2 were detected in both the cytoplasmic fraction and the nuclear fraction of the uninjected control and GFP dsRNA-injected control pupae at 72 h after larval-pupal ecdysis. Similar protein patterns were observed in *Ae. albopictus* (Figures 6A-2 and 6A-3) and *Cx. quinquefasciatus* (Figures 6C-2 and 6C-3) at 48 h after larval-pupal ecdysis. The protein level of putative cecropin B trimer in the cytoplasmic fraction was higher than that of the putative cecropin B nonamer (Figures 6A-2, 6B-2, and 6C-2). Similarly, in the nuclear fraction, the putative cecropin B nonamer was more abundant than the putative cecropin B trimer (Figures 6A-3, 6B-3, and 6C-3).

By way of contrast, in both the cytoplasmic and nuclear fractions of cecropin B dsRNA-injected pupae, the putative cecropin B trimers were significantly decreased in *Ae. albopictus* (Figures 6A-2 and 6A-3) and *Cx. quinquefasciatus* (Figures 6C-2 and 6C-3) at 48 h after larval-pupal ecdysis, and in *Ar. subalbatus* at 72 h after larval-pupal ecdysis (Figures 6B-2 and 6B-3). Furthermore, only a small amount of the putative cecropin B nonamer was detected in the cytoplasmic and nuclear fractions of the cecropin B dsRNA-injected pupae in *Ae. albopictus* (Figures 6A-2 and 6A-3) and *Cx. quinquefasciatus* (Figures 6C-2 and 6C-3) at 48 h after larval-pupal ecdysis, and in *Ar. subalbatus* (Figures 6B-2 and 6B-3) at 72 h after larval-pupal ecdysis. Overall, the cecropin B protein patterns of *Ae. albopictus*, *Ar. subalbatus*, and *Cx. quinquefasciatus* in the present study were very similar to those of Aacec B during the pupal stage of *Ae. aegypti*.
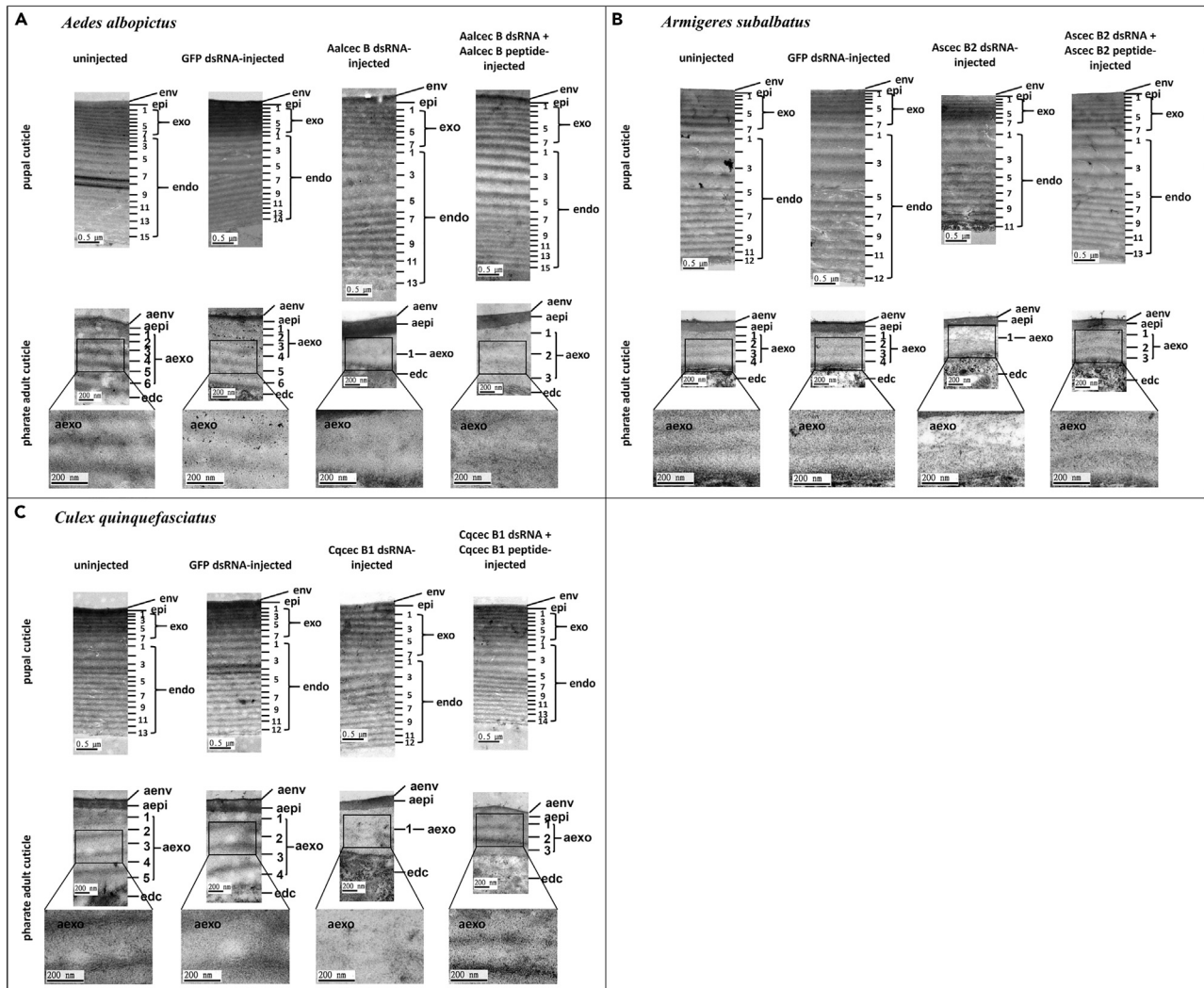
Figure 5. Ultrastructural observations of the pupal cuticle and pharate adult cuticle of the uninjected control, GFP dsRNA-injected control, surviving cecropin B dsRNA-injected pupae, and surviving pupae injected simultaneously with cecropin B dsRNA and cecropin B peptide

(A) *Aedes albopictus*, (B) *Armigeres subalbatus*, and (C) *Culex quinquefasciatus*. Env: envelope, epi: epicuticle, exo: exocuticle, endo: endocuticle, edc: epidermal cell, aenv: pharate adult envelope, aepi: pharate adult epicuticle, aexo: pharate adult exocuticle. The time point of the ultrastructural observations in (A) *Aedes albopictus* and (C) *Culex quinquefasciatus* was 48 h after larval-pupal ecdysis, and (B) in *Ar. subalbatus* was 72 h after larval-pupal ecdysis. The boxed figures are higher magnifications of the pharate adult exocuticle showing the helicoidal pattern of the chitin microfibrils. Note that, when the uninjected control and GFP dsRNA-injected control mosquitoes were examined, the pupal cuticle consisted of an envelope, an epicuticle, a laminated exocuticle, and a laminated endocuticle. By way of contrast, the pharate adult cuticle consisted of an envelope, an epicuticle, and one laminated exocuticle. The lamellae of the pharate adult exocuticle of the uninjected control and GFP dsRNA-injected control (A) from *Ae. albopictus* consisted of six lamellae, (B) from *Ar. subalbatus* consisted of four lamellae, and (C) from *Culex quinquefasciatus* consisted of five lamellae. Furthermore, the chitin microfibrils in the controls were arranged in a helicoidal pattern giving a fully formed exocuticle lamellae. In contrast, only one-laminated exocuticle is present in the pharate adult cuticle of the surviving cecropin B dsRNA-injected pupae. The chitin microfibrils are disorganized and do not form a helicoidal pattern. In pupae injected simultaneously with cecropin B dsRNA and cecropin B peptide, the exocuticle of the pharate adult cuticle consists of three lamellae with an arranged helicoidal pattern of the chitin microfibrils.

Injection of synthetic cecropin B peptide into pupae of *Ae. albopictus*, *Ar. subalbatus*, and *Cx. quinquefasciatus* elevates the transcription levels of PPO 3

The above findings demonstrate that knockdown of cecropin B in pupae results in a high mortality (Figures 2D–2F), the emergence of deformed adults, an impairment of pharate adult cuticle formation (Figure 5), and a reduction in the transcription of PPO 3 (Figure 4). We therefore hypothesize that these three cecropin B molecules are involved in regulating the expression of the relevant PPO 3 genes in these three mosquito species. As shown in Figure 7, the expression level of AalPPO 3 in pupae of *Ae. albopictus*
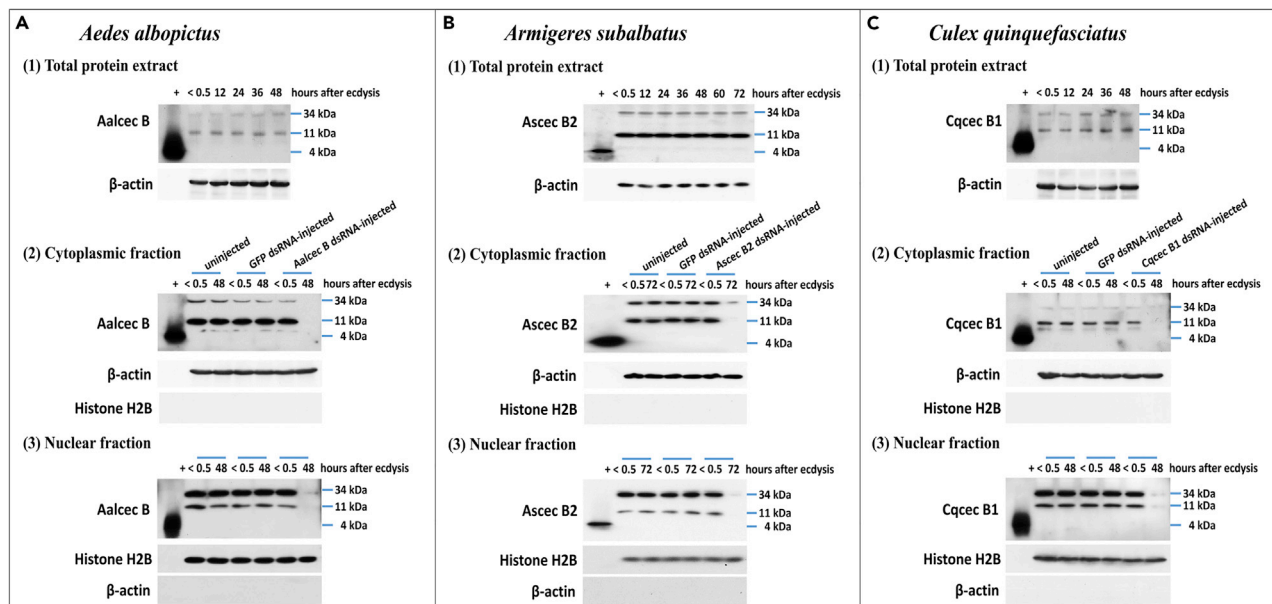
Figure 6. Western blot analysis reveals the presence of cecropin B peptides in the pupal cells

(A) *Aedes albopictus* cecropin B (Aalcec B), (B) *Armigeres subalbatus* cecropin B2 (Ascec B2), and (C) *Culex quinquefasciatus* cecropin B1 (Cqcec B1) in (1) total protein samples, (2) cytoplasmic fractions, and (3) nuclear fractions from the pupal cells of *Ae. albopictus*, *Ar. subalbatus*, and *Cx. quinquefasciatus*, respectively. β-actin and histone H2B were used as loading controls for the cytoplasmic and nuclear fractions, respectively. < 0.5–72: <0.5–72 h after injection. +: 1 ng synthetic peptide of Aalcec B, Ascec B2, or Cqcec B1.

injected with Aalcec B peptide was elevated at 12, 24, 36, and 48 h (Figure 7A). Similarly, an elevation of the expression level of As-pro-PO III was observed in the pupae of *Ar. subalbatus* at 12, 24, 36, 48, and 72 h after injection with Ascec B2 peptide (Figure 7B). Finally, an elevation of the expression level of CqPPO 3 in the pupae of *Cx. quinquefasciatus* was observed at 24, 36, and 48 h after injection with Cqcec B1 peptide (Figure 7C).

Cecropin B peptide binds *in vivo* to TTGGCA and to TTGGAA motifs within the PPO 3 DNA of *Ae. albopictus*, *Ar. subalbatus*, and *Cx. quinquefasciatus*

The above findings indicated that synthetic cecropin B induced expression of PPO 3 in pupae of *Ae. albopictus*, *Ar. subalbatus*, and *Cx. quinquefasciatus* (Figure 7). Liu et al. (2017) demonstrated that the Aacec B peptide binds directly *in vivo* to a TTGG(A/C)A motif that is present in AaPPO 3 DNA. As shown in Figure 8A, the exon-intron gene structures of both AalPPO 3 and As-pro-PO III are composed of five exons separated by four short introns, which is similar to that of AaPPO 3 (Liu et al., 2017). Two highly conserved copper-binding sites, Cu A and Cu B, are situated in exons II and III, respectively. On the other hand, CqPPO 3 is composed of only four exons, which are separated by three short introns; in this case, Cu A and Cu B are situated in exons I and II, respectively. Sequence analysis found that eight TTGG(A/C)A motifs were present in AalPPO 3, seven in As-pro-PO III, and four in CqPPO 3. Next, we used chromatin immunoprecipitation (ChIP) assays to determine whether the cecropin B peptides are able to bind to the *Ae. albopictus*, *Ar. subalbatus*, and *Cx. quinquefasciatus* PPO 3 DNA fragments containing the TTGG(A/C)A putative binding motifs. As shown in Figure 8B, as compared with controls, the 5′ end-2, the 5′ end-3, the copper-binding site A (Cu A), Exon II (E II), and the copper-binding site B (Cu B) fragments from AalPPO 3 DNA were significantly enriched in the ChIP fractions. Furthermore, the 5′ end-2 and the Cu B of As-pro-PO III DNA fragments and Exon III (E III)-1 and E III-2 of CqPPO 3 DNA fragments, all of which contain a TTGGCA motif, were also significantly enriched (Figure 8B). Subsequently, qPCR was used to analyze the interaction of cecropin B with the PPO 3 DNA fragments containing either a TTGGAA motif or a TTGGCA motif. As shown in Figure 8C, the signals from the TTGG(C/A)A motif in the 5′ end-2, 5′ end-3, Cu A, E II, and Cu B DNA fragments of AalPPO 3 could be detected at 12 h after larval-pupal ecdysis, then this signal was slightly decreased at 24 h after ecdysis; following this, the signals of the 5′ end-2, Cu A, E II, and Cu B DNA fragments significantly increased at 48 h after ecdysis. Somewhat differently, the signal from the TTGGCA motif in the 5′ end-3 DNA fragment was significantly increased at 36 h after larval-pupal ecdysis and then
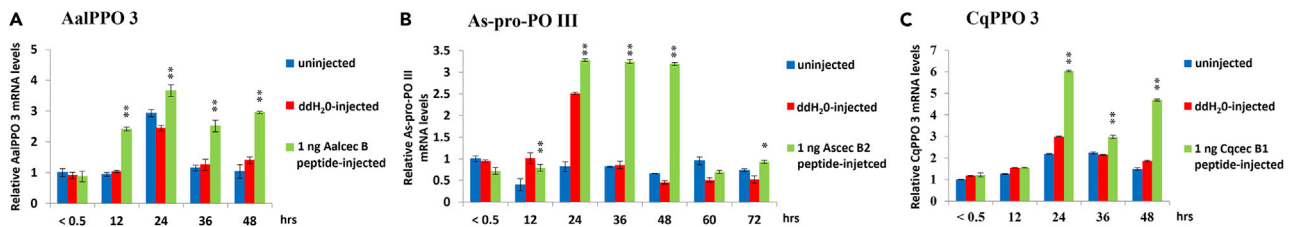
Figure 7. Synthetic cecropin B peptide is able to enhance the transcription levels of PPO 3 in pupae

qPCR results were normalized against the mRNA expression of *Ae. albopictus* ribosomal protein L32 (AalRPL32), *Ar. subalbatus* ribosomal protein S7 (AsS7), and *Cx. quinquefasciatus* ribosomal protein S7 (CqS7), respectively. Values are means $\pm$ SD, n = 3. Asterisks indicate significant differences (*p < 0.005; **p < 0.001) compared to the relative mRNA levels of the uninjected control at each time point.

(A) The transcription levels of AalPPO 3 in the uninjected control pupae, the H_2O-injected control pupae, and the Aalcec B peptide-injected pupae of *Ae. albopictus*.

(B) The transcription levels of As-pro-PO III in the uninjected control pupae, the H_2O-injected control pupae, and the Ascec B2 peptide-injected pupae of *Ar. subalbatus*.

(C) The transcription levels of CqPPO 3 in the uninjected control pupae, the H_2O-injected control pupae, and the Cqcec B1 peptide-injected pupae of *Cx. quinquefasciatus*.

was found to have decreased at 48 h after ecdysis. Using As-pro-PO-III, the signals from the TTGGCA motif in the 5′ end-2 and Cu B DNA fragments were detected immediately after larval-pupal ecdysis, and were increased at 12 h after larval-pupal ecdysis, which was then followed by a decrease to a low level at 24 h after larval-pupal ecdysis; thereafter, this was followed by a gradual increase from 36 to 72 h after larval-pupal ecdysis. Furthermore, the increase in the signal related to the Cu B DNA fragment was higher than the signal related to the 5′ end-2 DNA fragment at both <0.5 and 48 h after larval-pupal ecdysis. Using CqPPO 3, the signals from the TTGGCA motif within the E III-1 and E III-2 DNA fragments were detected at 12 h after ecdysis, and these were increased significantly at 24 h after ecdysis and then decreased to low levels at 36–48 h after ecdysis. The signal related to the E III-2 DNA fragment was higher than the signal related to the E III-1 fragment (Figure 8C).

Cecropin B peptide binds *in vitro* to the *Ae. albopictus*, *Ar. subalbatus*, and *Cx. quinquefasciatus* PPO 3 DNA fragments containing the TTGG(A/C)A putative binding motifs

Subsequently, direct binding of the three cecropin B peptide to the AalPPO 3, As-pro-PO-III, and CqPPO 3 DNA fragments *in vitro* was investigated by DNA pull-down assay. PPO 3 DNA fragments containing the TTGG(A/C)A putative binding motifs were generated by cloning of the relevant DNA fragments followed by PCR amplification. As shown in Figure 9, Aalcec B directly binds the 5′ end-2, 5′ end-3, Cu A, E II, and Cu B DNA fragments of AalPPO 3 *in vitro*. Furthermore, Ascec B2 directly binds the 5′ end-2 and Cu B DNA fragments of As-pro-PO III. Finally, Cqcec B1 directly binds the E III-1 and E III-2 DNA fragments of CqPPO 3.

DISCUSSION

AMPs play a pivotal role in the innate immune responses of vertebrates (Zhang and Gallo, 2016; Riera Romo et al., 2016) and invertebrates (Bulet et al., 2004; Otero-González et al., 2010). Initially, AMPs were known as bactericidal peptides (Hultmark et al., 1980; Stotz et al., 2009; Klüver et al., 2006; Ganz, 2003; Schmitt et al., 2010), but recently certain AMPs have been found to be multi-functional. For example, β-defensin participates in sperm maturation and fertility in rats, mice, and humans (Semple and Dorin, 2012; Hu et al., 2014), while human cathelicidin LL-37/hCAP-18 directly activates angiogenesis by increasing the proliferation of endothelial cells (Koczulla et al., 2003; Wang et al., 2016); in addition, mouse orexin B enhances phagocytosis via activation of calcium-dependent potassium channels in peritoneal macrophages (Ichinose et al., 1998; Ohta et al., 2011). In insects, cecropins are the major family of inducible antibacterial peptides and have been shown to have a broad spectrum of antimicrobial activity (Hillyer, 2010). Liu et al. (2017) have demonstrated that Aacec B plays a crucial role in pharate adult cuticle formation by *Ae. aegypti* pupae via its regulation of AaPPO 3 gene expression. The results of the present study demonstrate that three other mosquito cecropin B molecules, namely Aalcec B, Ascec B2, and Cqcec B1, play similar roles in the cecropin-prophenoloxidase regulatory mechanisms present in *Ae. albopictus*, *Ar. subalbatus*, and *Cx. quinquefasciatus*, respectively. We found that five of the characteristics of the above three cecropin B molecules are remarkably similar to those of Aacec B from *Ae. aegypti*. These are: (1) the expression level
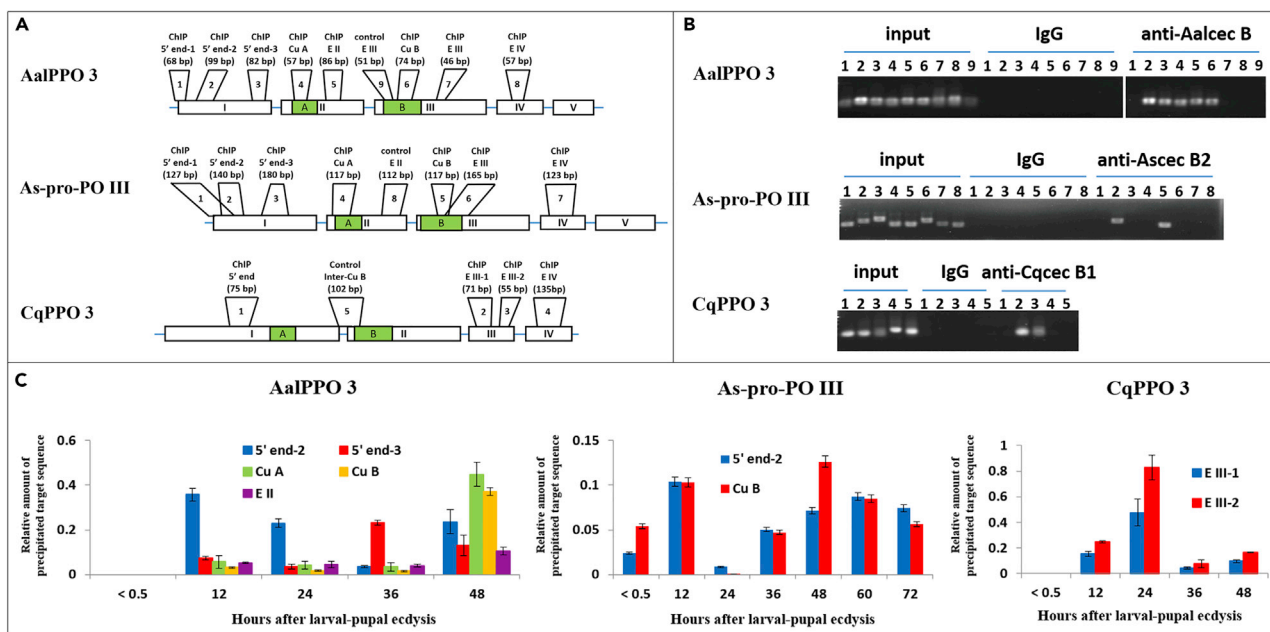
Figure 8. The ChIP assays reveal that cecropin B peptide *in vivo* binds to the TTGG(A/C)A putative binding motifs within the PPO 3 DNA fragments of the mosquito pupae

(A) Schematic representation of the ChIP and control primers. Open boxes with Roman numerals indicate exons. Numbers indicate the position of the PPO 3 DNA fragments containing the TTGG(A/C)A putative binding motifs. The green box represents the positions of copper-binding site A and B.

(B) The ChIP assays of the PPO 3 DNA fragments containing the TTGG(A/C)A putative binding motifs and one control fragment without the TTGG(A/C)A putative binding motif. Anti-Ascec B2 antibody was used for the ChIP assay. Normal rabbit IgG and control DNA fragment were used in this experiment as negative controls. Input DNA samples and ChIP fractions at < 0.5–72 h after larval-pupal ecdysis were mixed together to examine the specific binding of cecropin B peptide to the PPO 3 DNA fragments. Three independent experiments were carried out and gave similar results. The results from one experiment are shown.

(C) qPCR of the ChIP assay. Three independent experiments were done and gave similar results, each with triple biological repeats. The results shown are from one experiment with three technical replicates. Values are means ± SD, n = 3.

fluctuation of Aalcec B, Ascec B2, and Cqcec B1 in pupae (Figures 2A–2C); (2) the effects of knockdown on Aalcec B, Ascec B2, and Cqcec B1 in pupae of *Ae. albopictus*, *Ar. subalbatus*, and *Cx. quinquefasciatus* are similar to Aacec B-knockdown in *Ae. aegypti* pupae, namely a high pupal mortality (Figures 2D–2F and S3), a reduction in the transcription of PPO 3 (Figure 4), and an impairment of pharate adult cuticle formation (Figures 5 and S4); (3) multimeric forms of cecropin B are detectable in the cell nuclei of the pupae of the various species (Figure 6); (4) cecropin B is able to elevate directly or indirectly the transcription of PPO 3 in the three species (Figure 7); and (5) cecropin B binds *in vivo* to the putative TTGG(A/C)A binding motifs, which are present in multiple copies in PPO 3 DNA (Figure 8).

Although the roles of Aacec B, Aalcec B, Ascec B2, and Cqcec B1 seem to be similar during pharate adult cuticle formation, the time and intensity of cecropin B binding to the TTGG(A/C)A motif differs when *Ae. albopictus*, *Ar. subalbatus*, *Cx. quinquefasciatus* (Figure 8C), and *Ae. aegypti* are compared (Liu et al., 2017). These results suggest that each mosquito species requires a different response time when initiating the process of pharate adult cuticle formation. Liu et al. (2017) demonstrated that Aacec B binds to four putative motif TTGG(A/C)A within the DNA fragments that make up AaPPO 3. In the present study, we found that both Ascec B2 and Cqcec B1 bind to two putative binding motifs, while Aalcec B binds to five putative binding motif (Figure 8B). One possible explanation for this is the absence of the TTGGAA putative binding motif from the Cu B DNA fragments of both As-pro-PO III and CqPPO 3 (Figure S5B). Although the TTGGCA binding motif is presented within the Cu A DNA fragment of As-pro-PO III (Figure S5A), it would seem that Ascec B2 is unable to bind to this motif.

The nucleotide sequence of the putative binding motif TTGG(A/C)A is nearly identical to that of the consensus motif TTGGAA in the promoter region of the β-D-glucosidase I gene of *Bifidobacterium breve* 203 (Nunoura et al., 1997) and that of the consensus motif TTGGCA of the eukaryotic nuclear factor I (NFI)
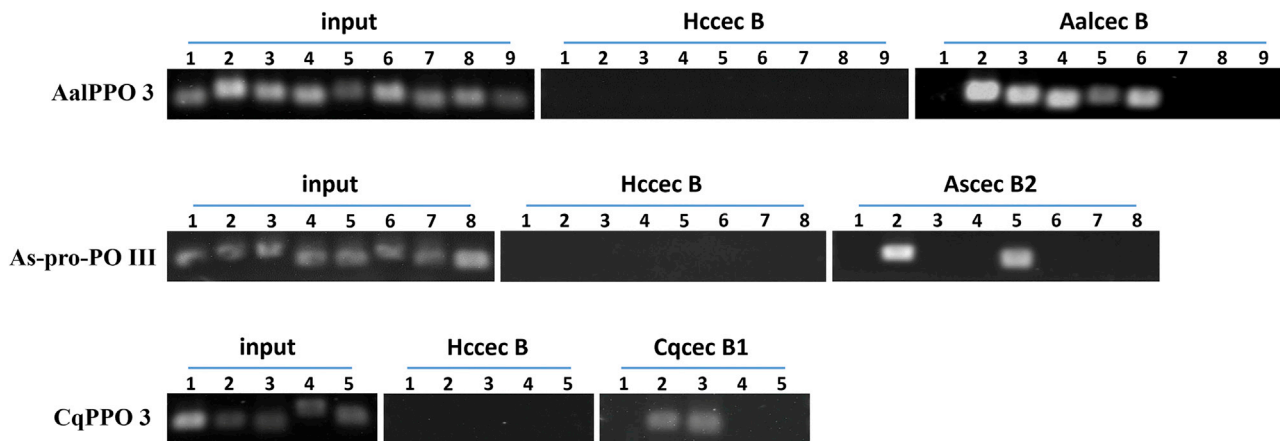
Figure 9. DNA pull-down assay showing that cecropin B peptide binds directly to the PPO 3 DNA fragments of the mosquito pupae
The figures show the PCR analyses of the PPO 3 DNA fragments that bind to cecropin B-conjugated beads. Hccec B-conjugated beads were used as controls. Three independent experiments were done and gave similar results, each with triple biological repeats. The results shown are from one experiment with three technical replicates.

family transcription factors (Osada et al., 1996), which are essential for mammalian development (Gronostajski, 2000; Whittle et al., 2009). Therefore, it is reasonable to assume that the TTGG(A/C)A motifs in PPO 3 are functional and are involved in the regulating the expression of this development-related gene during pupal development in mosquitoes. In the last decade, PPO 3 has been suggested to be a critical enzyme in the melanization reaction in *Ae. aegypti* (Wang et al., 2017) and *Drosophila melanogaster* (Dudzic et al., 2015), as well as in the cuticle formation of *Ar. subalbatus* (Tsao et al., 2010) and *Ae. aegypti* (Liu et al., 2017). Although the exon-intron gene structure of CqPPO 3 is different from that of AaPPO 3 (Liu et al., 2017), AalPPO 3, and As-pro-PO III (Figure 4A), all of the gene expression and the physiological functions of the four PPO 3 genes are similar during the pupal metamorphosis of *Ae. aegypti*, *Ae. albopictus*, *Ar. subalbatus*, and *Cx. quinquefasciatus*. Thus, it would be interesting to further elucidate in more detail how PPO 3 is activated during pupal development in mosquitoes.

The molting process and metamorphosis of insects are coordinately regulated by two major hormones, these are the sesquiterpenoid juvenile hormone (JH) and the steroid 20-hydroxyecdysone (20E) (Dubrovsky, 2005). JH determines the nature of the molt, while 20E initiates and orchestrates larval-larval molting and larval-pupal-adult metamorphosis (Tian et al., 2010; Liu et al., 2018). During the onset of metamorphosis, 20E initiates various early gene expression cascades and induces the formation of the pupal cuticle in order to regulate the insect's developmental transitions (Dong et al., 2003; King-Jones et al., 2005; Yamanaka et al., 2013). Previous studies have demonstrated that 20E modulates the cellular and humoral innate immunity of insects (Flatt et al., 2008; Tian et al., 2010; Sun et al., 2016) by priming the production of various effector genes, including cecropins (Reynolds et al., 2020; Nunes et al., 2020) and PPOs (Han et al., 2020; Reynolds et al., 2020). The results of Liu et al. (2017) and of the present study demonstrate that, in *Ae. aegypti*, *Ae. albopictus*, *Ar. subalbatus*, and *Cx. quinquefasciatus*, cecropin B is expressed constitutively and regulates the transcription of PPO 3 in wild-type pupae. The precise regulatory mechanism controlling cecropin B-PPO 3 in mosquitoes still remains unclear, and therefore further experiments are necessary to test whether 20E orchestrate cuticle formation via the cecropin-prophenoloxidase regulatory mechanism during metamorphosis in insects. Zufelato et al. (2004) have shown that 20E activates the transcription of PPO in *Apis mellifera* (Hymenoptera: Apidae). Because no homolog of Aacec B is present in hymenopteran and hemipteran insects, it would also be interesting to study how 20E regulates the PPO cascade in hymenopteran and hemipteran insects.

Double-stranded RNA-mediated interference (RNAi) is a widely used tool for the artificially manipulating gene expression in many organisms (Liu et al., 2010; Zhao et al., 2016). However, it may produce off-target effects. In order to validate precisely RNAi-induced phenotypes, the ideal method is through rescue of the RNAi phenotype by the targeted gene itself (Schulz et al., 2009) or via cross-species rescue by expressing an orthologous gene from a closely related species (Kondo et al., 2009). Results of the present study demonstrated that all of the knockdowns of cecropin B were cross-species rescued by synthetic

sequence-similar cecropin B peptides from other mosquito species, indicating that RNAi rescue with a homologous synthetic peptide in *Ae. aegypti*, *Ae. albopictus*, *Ar. subalbatus*, and *Cx. quinquefasciatus* is achieved using a cross-species approach.

In conclusion, the present study has demonstrated that three mosquito cecropins, Aalcec B, Ascec B2, and Cqcec B1, all play a significant role in the pharate adult cuticle formation in pupae of *Ae. albopictus*, *Ar. subalbatus*, and *Cx. quinquefasciatus* via the regulation of AalPPO 3, As-pro-PO III, and CqPPO 3, respectively. The results of this study support the idea that the cecropin-prophenoloxidase regulatory mechanisms are active during cuticle formation is a cross-species manner in these three species of mosquitoes. Further studies in the future should be carried out to determine whether the cecropin-prophenoloxidase regulatory mechanism during cuticle formation is a conserved mechanism in other insects.

Limitations of study

Our findings show that the three cecropin B genes studied here are homologes of Aacec B and that they play a similar crucial role in the cecropin-prophenoloxidase regulation mechanism during pupal development. It would be of great interest to explore whether cecropins that have a more distant evolutionary relationship than the above three genes also participate in cecropin-prophenoloxidase regulation.

STAR★METHODS

Detailed methods are provided in the online version of this paper and include the following:

- KEY RESOURCES TABLE
- RESOURCE AVAILABILITY
  - Lead contact
  - Materials availability
  - Data and code availability
- EXPERIMENTAL MODEL AND SUBJECT DETAILS
  - Mosquito rearing
  - Double-stranded RNA synthesis and injection
  - Ethics approval and consent to participate
- METHOD DETAILS
  - Sequence alignment and phylogenetic analysis
  - RNA extraction
  - Reverse transcription-quantitative PCR (RT-qPCR) analysis
  - Protein synthesis
  - SDS-polyacrylamide gel electrophoresis (SDS-PAGE) and western blotting
  - Transmission electron microscopy (TEM)
  - Standard and quantitative chromatin immunoprecipitation (standard ChIP and qChIP)
  - DNA pull-down assay
- QUANTIFICATION AND STATISTICAL ANALYSIS

SUPPLEMENTAL INFORMATION

Supplemental information can be found online at https://doi.org/10.1016/j.isci.2022.104478.

AUTHOR CONTRIBUTIONS

WTL designed, performed the experiments, produced the images of TEM, and wrote the paper. DDJ supervised the experiments. WCT supervised the project and designed the experiments. CCC supervised the project, designed the experiments, and wrote the paper. All authors contributed to the manuscript.

REFERENCES

Bulet, P., Stöcklin, R., and Menin, L. (2004). Antimicrobial peptides: from invertebrates to vertebrates. Immunol. Rev. *198*, 169–184. https://doi.org/10.1111/j.0105-2896.2004.0124.x.

Cho, W.L., Liu, H.S., Lee, C.H., Kuo, C.C., Chang, T.Y., Liu, C.T., and Chen, C.C. (1998). Molecular cloning, characterization and tissue expression of prophenoloxidase cDNA from the mosquito *Armigeres subalbatus* inoculated with *Dirofilaria immitis* microfilariae. Insect Mol. Biol. *7*, 31–40. https://doi.org/10.1046/j.1365-2583.1998.71049.x.

Costa, C.P., Elias-Neto, M., Falcon, T., Dallacqua, R.P., Martins, J.R., and Bitondi, M.M.G. (2016). RNAi-mediated functional analysis of bursicon genes related to adult cuticle formation and tanning in the honeybee, *Apis mellifera*. PLoS One *11*, e0167421. https://doi.org/10.1371/journal.pone.0167421.

Dong, Y., Dinan, L., and Friedrich, M. (2003). The effect of manipulating ecdysteroid signaling on embryonic eye development in the locust *Schistocerca americana*. Dev. Genes Evol. *213*, 587–600. https://doi.org/10.1007/s00427-003-0367-z.

Dubrovsky, E.B. (2005). Hormonal cross talk in insect development. Trends Endocrinol. Metab. *16*, 6–11. https://doi.org/10.1016/j.tem.2004.11.003.

Dudzic, J.P., Kondo, S., Ueda, R., Bergman, C.M., and Lemaitre, B. (2015). *Drosophila* innate immunity: regional and functional specialization of prophenoloxidases. BMC Biol. *1*, 81.

Flatt, T., Heyland, A., Rus, F., Porpiglia, E., Sherlock, C., Yamamoto, R., Garbuzov, A., Palli, S.R., Tatar, M., and Silverman, N. (2008). Hormonal regulation of the humoral innate immune response in *Drosophila melanogaster*. J. Exp. Biol. *211*, 2712–2724. https://doi.org/10.1242/jeb.014878.

Ganz, T. (2003). Defensins: antimicrobial peptides of innate immunity. Nat. Rev. Immunol. *3*, 710–720. https://doi.org/10.1038/nri1180.

Gronostajski, R.M. (2000). Roles of the NFI/CTF gene family in transcription and development. Gene *249*, 31–45. https://doi.org/10.1016/s0378-1119(00)00140-2.

Han, P., Gong, Q., Fan, J., Zhang, M., Abbas, M., Zhu, W., Deng, S., Xing, S., and Zhang, J. (2020). 20-hydroxyecdysone regulates the prophenoloxidase cascade to immunize *Metarhizium anisopliae* in *Locusta migratoria*. Pest Manag. Sci. *76*, 3149–3158. https://doi.org/10.1002/ps.5869.

Hillyer, J.F. (2010). Mosquito immunity. Adv. Exp. Med. Biol. *708*, 218–238. https://doi.org/10.1007/978-1-4419-8059-5_12.

Hu, S.G., Zou, M., Yao, G.X., Ma, W.B., Zhu, Q.L., Li, X.Q., Chen, Z.J., and Sun, Y. (2014). Androgenic regulation of beta-defensins in the mouse epididymis. Reprod. Biol. Endocrinol. *12*, 76. https://doi.org/10.1186/1477-7827-12-76.

Huang, L.H., Christensen, B.M., and Chen, C.C. (2001). Molecular cloning of a second prophenoloxidase cDNA from the mosquito *Armigeres subalbatus*: prophenoloxidase expression in blood-fed and microfilariae-inoculated mosquitoes. Insect Mol. Biol. *10*, 87–96. https://doi.org/10.1046/j.1365-2583.2001.00241.x.

Hultmark, D., Steiner, H., Rasmuson, T., and Boman, H.G. (1980). Insect immunity: purification and properties of three inducible bactericidal proteins from hemolymph of immunized pupae of *Hyalophora cecropia*. Eur. J. Biochem. *106*, 7–16. https://doi.org/10.1111/j.1432-1033.1980.tb05991.x.

Ichinose, M., Asai, M., Sawada, M., Sasaki, K., and Oomura, Y. (1998). Induction of outward current by orexin-B in mouse peritoneal macrophages. FEBS Lett. *440*, 51–54. https://doi.org/10.1016/s0014-5793(98)01432-x.

Liu, S., Ding, Z., Zhang, C., Yang, B., and Liu, Z. (2010). Gene knockdown by intro-thoracic injection of double-stranded RNA in the brown planthopper, *Nilaparvata lugens*. Insect Biochem. Mol. Biol. *40*, 666–671. https://doi.org/10.1016/j.ibmb.2010.06.007.

Liu, S., Li, K., Gao, Y., Liu, X., Chen, W., Ge, W., Feng, Q., Palli, S.R., and Li, S. (2018). Antagonistic actions of juvenile hormone and 20-hydroxyecdysone within the ring gland determine developmental transitions in *Drosophila*. Proc. Natl. Acad. Sci. U S A *115*, 139–144. https://doi.org/10.1073/pnas.1716897115.

Liu, W.T., Tu, W.C., Lin, C.H., Yang, U.C., and Chen, C.C. (2017). Involvement of cecropin B in the formation of the *Aedes aegypti* mosquito cuticle. Sci. Rep. *7*, 16395. https://doi.org/10.1038/s41598-017-16625-6.

Liu, W.T., Chen, T.L., Hou, R.F., Chen, C.C., and Tu, W.C. (2020). The invasion and encapsulation of the entomopathogenic nematode, *Steinernema abbasi*, in *Aedes albopictus* (Diptera: Culicidae) larvae. Insects *11*, 832. https://doi.org/10.3390/insects11120832.

Locke, M., and Krishnan, N. (1971). The distribution of phenoloxidases and polyphenols during cuticle formation. Tissue Cell *3*, 103–126. https://doi.org/10.1016/s0040-8166(71)80034-4.

King-Jones, K., Charles, J.P., Lam, G., and Thummel, C.S. (2005). The ecdysone-induced DHR4 orphan nuclear receptor coordinates growth and maturation in *Drosophila*. Cell *121*, 773–784. https://doi.org/10.1016/j.cell.2005.03.030.

Klüver, E., Adermann, K., and Schulz, A. (2006). Synthesis and structure-activity relationship of beta-defensins, multi-functional peptides of the immune system. J. Pept. Sci. *12*, 243–257. https://doi.org/10.1002/psc.749.

Kondo, S., Booker, M., and Perrimon, N. (2009). Cross-species RNAi rescue platform in *Drosophila melanogaster*. Genetics *183*, 1165–1173. https://doi.org/10.1534/genetics.109.106567.

Koczulla, R., von Degenfeld, G., Kupatt, C., Krötz, F., Zahler, S., Gloe, T., Issbrücker, K., Unterberger, P., Zaiou, M., Lebherz, C., et al. (2003). An angiogenic role for the human peptide antibiotic LL-37/hCAP-18. J. Clin. Invest. *111*, 1665–1672. https://doi.org/10.1172/jci17545.

Marinotti, O., Ngo, T., Kojin, B.B., Chou, S.P., Nguyen, B., Juhn, J., Carballar-Lejarazú, R., Marinotti, P.N., Jiang, X., Walter, M.F., et al. (2014). Integrated proteomic and transcriptomic analysis of the *Aedes aegypti* eggshell. BMC Dev. Biol. *14*, 15. https://doi.org/10.1186/1471-213x-14-15.

Nunes, C., Sucena, É., and Koyama, T. (2020). Endocrine regulation of immunity in insects. FEBS J. *288*, 3928–3947. https://doi.org/10.1111/febs.15581.

Nunoura, N., Ohdan, K., Yamamoto, K., and Kumagai, H. (1997). Expression of the β-d-glucosidase I gene in *Bifidobacterium breve* 203 during acclimation to cellobiose. J. Ferment. Bioeng. *83*, 309–314. https://doi.org/10.1016/s0922-338x(97)80134-1.

Ohta, K., Kajiya, M., Zhu, T., Nishi, H., Mawardi, H., Shin, J., Elbadawi, L., Kamata, N., Komatsuzawa, H., and Kawai, T. (2011). Additive effects of orexin B and vasoactive intestinal polypeptide on LL-37-mediated antimicrobial activities. J. Neuroimmunol. *233*, 37–45. https://doi.org/10.1016/j.jneuroim.2010.11.009.

Osada, S., Daimon, S., Nishihara, T., and Imagawa, M. (1996). Identification of DNA binding-site preferences for nuclear factor I-A. FEBS Lett. *390*, 44–46. https://doi.org/10.1016/0014-5793(96)00622-9.

Otero-Gonzáiez, A.J., Magalhães, B.S., Garcia-Villarino, M., López-Abarrategui, C., Sousa, D.A.,

Dias, S.C., and Franco, O.L. (2010). Antimicrobial peptides from marine invertebrates as a new Frontier for microbial infection control. FASEB J. *24*, 1320–1334. https://doi.org/10.1096/fj.09-143388.

Reynolds, R.A., Kwon, H., and Smith, R.C. (2020). 20-hydroxyecdysone primes innate immune responses that limit bacterial and malarial parasite survival in *Anopheles gambiae*. mSphere *5*, e00983-19. https://doi.org/10.1128/msphere.00983-19.

Riera Romo, M., Pérez-Martínez, D., and Castillo Ferrer, C. (2016). Innate immunity in vertebrates: an overview. Immunology *148*, 125–139. https://doi.org/10.1111/imm.12597.

Schmitt, P., Wilmes, M., Pugnière, M., Aumelas, A., Bachère, E., Sahl, H.G., Schneider, T., and Destoumieux-Garzón, D. (2010). Insight into invertebrate defensin mechanism of action: oyster defensins inhibit peptidoglycan biosynthesis by binding to lipid II. J. Biol. Chem. *285*, 29208–29216. https://doi.org/10.1074/jbc.m110.143388.

Schulz, J.G., David, G., and Hassan, B.A. (2009). A novel method for tissue-specific RNAi rescue in *Drosophila*. Nucleic. Acids Res. *37*, e93. https://doi.org/10.1093/nar/gkp450.

Semple, F., and Dorin, J.R. (2012). β-Defensins: multifunctional modulators of infection, inflammation and more? J. Innate Immun. *4*, 337–348. https://doi.org/10.1159/000336619.

Shiao, S.H., Higgs, S., Adelman, Z., Christensen, B.M., Liu, S.H., and Chen, C.C. (2001). Effect of prophenoloxidase expression knockout on the melanization of microfilariae in the mosquito *Armigeres subalbatus*. Insect Mol. Biol. *10*, 315–321. https://doi.org/10.1046/j.0962-1075.2001.00268.x.

Stotz, H.U., Thomson, J.G., and Wang, Y. (2009). Plant defensins: defense, development and application. Plant Signal. Behav. *4*, 1010–1012. https://doi.org/10.4161/psb.4.11.9755.

Suderman, R.J., Dittmer, N.T., Kanost, M.R., and Kramer, K.J. (2006). Model reactions for insect cuticle sclerotization: cross-linking of recombinant cuticular proteins upon their laccase-catalyzed oxidative conjugation with catechols. Insect Biochem. Mol. Biol. *36*, 353–365. https://doi.org/10.1016/j.ibmb.2006.01.012.

Sun, W., Shen, Y.H., Zhou, L.X., and Zhang, Z. (2016). Ecdysone titer determined by 3DE-3β-reductase enhances the immune response in the silkworm. J. Immunol. *196*, 1646–1654. https://doi.org/10.4049/jimmunol.1500158.

Tian, L., Guo, E., Diao, Y., Zhou, S., Peng, Q., Cao, Y., Ling, E., and Li, S. (2010). Genome-wide regulation of innate immunity by juvenile hormone and 20-hydroxyecdysone in the *Bombyx fat* body. BMC Genom. *11*, 549. https://doi.org/10.1186/1471-2164-11-549.

Tsao, I.Y., Chen, J.W., Li, C.J., Lo, H.L., Christensen, B.M., and Chen, C.C. (2015). The dual roles of *Armigeres subalbatus* prophenoloxidase V in parasite melanization and egg chorion melanization in the mosquito *Ar. subalbatus*. Insect Biochem. Mol. Biol. *64*, 68–77. https://doi.org/10.1016/j.ibmb.2015.07.016.

Tsao, I.Y., Christensen, B.M., and Chen, C.C. (2010). *Armigeres subalbatus* (Diptera: Culicidae) prophenoloxidase III is required for mosquito cuticle formation: ultrastructural study on dsRNA-knockdown mosquitoes. J. Med. Entomol. *47*, 495–503. https://doi.org/10.1093/jmedent/47.4.495.

Wang, W., Jia, J., Li, C., Duan, Q., Yang, J., Wang, X., Li, R., Chen, C., Yan, H., and Zheng, Y. (2016). Antimicrobial peptide LL-37 promotes the proliferation and invasion of skin squamous cell carcinoma by upregulating DNA-binding protein A. Oncol. Lett. *12*, 1745–1752. https://doi.org/10.3892/ol.2016.4865.

Wang, Y., Jiang, H., Cheng, Y., An, C., Chu, Y., Raikhel, A.S., and Zou, Z. (2017). Activation of *Aedes aegypti* prophenoloxidase-3 and its role in the immune response against entomopathogenic fungi. Insect Mol. Biol. *26*, 552–563. https://doi.org/10.1111/imb.12318.

Whittle, C.M., Lazakovitch, E., Gronostajski, R.M., and Lieb, J.D. (2009). DNA-binding specificity and in vivo targets of *Caenorhabditis elegans* nuclear factor I. Proc. Natl. Acad. Sci. U S A *106*, 12049–12054. https://doi.org/10.1073/pnas.0812894106.

Yamanaka, N., Rewitz, K.F., and O'Connor, M.B. (2013). Ecdysone control of developmental transitions: lessons from *Drosophila* research. Annu. Rev. Entomol. *58*, 497–516. https://doi.org/10.1146/annurev-ento-120811-153608.

Zhang, L.J., and Gallo, R.L. (2016). Antimicrobial peptides. Curr. Biol. *26*, R14–R19. https://doi.org/10.1016/j.cub.2015.11.017.

Zhao, L., Yang, M., Shen, Q., Liu, X., Shi, Z., Wang, S., and Tang, B. (2016). Functional characterization of three trehalase genes regulating the chitin metabolism pathway in rice brown planthopper using RNA interference. Sci. Rep. *6*, 27841. https://doi.org/10.1038/srep27841.

Zufelato, M.S., Lourenço, A.P., Simões, Z.L., Jorge, J.A., and Bitondi, M.M. (2004). Phenoloxidase activity in *Apis mellifera* honey bee pupae, and ecdysteroid-dependent expression of the prophenoloxidase mRNA. Insect Biochem. Mol. Biol. *34*, 1257–1268. https://doi.org/10.1016/j.ibmb.2004.08.005.

STAR★METHODS

KEY RESOURCES TABLE

REAGENT or RESOURCE	SOURCE	IDENTIFIER
Antibodies		
Anti-β-actin antibody	Santa Cruz Biotechnology Inc., USA	Cat# sc-47778 HRP, RRID:AB_271418
Secondary anti-mouse immunoglobulin-horseradish peroxidase	PerkinElmer, Inc., USA	NEF822
Anti-histone H2B (D2H6) antibody	Cell Signaling Technology, USA	Cat# 12364, RRID:AB_2714167
Secondary anti-rabbit immunoglobulin-horseradish peroxidase	KPL, USA	474-1516
anti-Ascec B2 antibody	Yao-Hong Biotechnology Inc., Taiwan	N/A
Chemicals, peptides, and recombinant proteins		
goose liver powder	NTN Fishing Bait LTD., Taiwan	N/A
yeast powder	Taiwan Sugar Corp., Taiwan	N/A
TRI Reagent®	Merck, USA	T9424
1-Bromo-3-chloropropane	Sigma-Aldrich, USA	B9673-200ML
2-propanol	Sigma-Aldrich, USA	278475
synthetic cecropin B peptides	Genemed Synthesis Inc., USA	N/A
5% β-mercaptoethanol	Sigma-Aldrich, USA	63689-25ML-F
Glutaraldehyde	Electron Microscopy Science, USA	cat. #16220
Cacodylate	Merck, USA	C0250
uranyl acetate	Bio-Rad, USA	a2312/3
lead citrate	Electron Microscopy Science, USA	cat. #17800
Formaldehyde	Sigma-Aldrich, USA	252549
Glycine	Sigma-Aldrich, USA	G-7126
Luminata™ Classico Western Chemiluminescent HRP Substrates	Merck, USA	WBLUC0500
MEGAscript™ T3 transcription kit	Thermo Scientific, USA	AM1338
MEGAscript™ T7 transcription kit	Thermo Scientific, USA	AMB1334
RevertAid™ First Strand cDNA Synthesis Kit	Thermo Scientific, USA	K1622
2x ChamQ Universal SYBR qPCR Master Mix	Vazyme Biotech, China	Q711
Epon 812 resin	Electron Microscopy Science, USA	EMS #14120
RevertAid™ First Strand cDNA Synthesis Kit	Thermo Scientific, USA	K1622
Pierce™ Magnetic ChIP Kit	Thermo Scientific, USA	26157
Experimental models: Organisms/strains		
Mouse: ICR	National Taiwan University College of Medicine Laboratory Animal Center	N/A
Oligonucleotides		
PCR primers	Mission Biotech Co. Ltd., Taiwan	See Table S1 for a list of oligonucleotides
Software and algorithms		
Clustal Omega	EMBL-EBI	https://www.ebi.ac.uk/Tools/msa/clustalo/
Adobe Photoshop	Photoshop Software	https://www.adobe.com
MEGA-X	Mega software	https://www.megasoftware.net/
The MEME Suite	MEME	https://meme-suite.org/meme/

Continued

REAGENT or RESOURCE	SOURCE	IDENTIFIER
GraphPad Prism Software	GraphPad	https://www.graphpad.com/scientific software/prism/
Other		
NCBI	NIH	http://www.ncbi.nlm.nih.gov/
Triatoma Transcriptomes	N/A	http://201.131.57.23:8080/data/triatoma
Ensembl Genomes	EMBL-EBI	http://ensemblgenomes.org/
AphidCyc	Université de Lyon	http://acypicyc.cycadsys.org/
Hymenoptera Genome Database	University of Missouri	https://hymenoptera.elsiklab.missouri.edu/

RESOURCE AVAILABILITY

Lead contact

Further information and requests for resources and reagents should be directed to and will be fulfilled by the lead contact, Wu-Chun Tu (wctu@dragon.nchu.edu.tw).

Materials availability

This study did not generate new unique reagents.

Data and code availability

This paper analyzes existing publicly available data, with information in the key resources table. This paper does not report any original code. Any additional information required to reanalyze the data reported in this paper is available from the lead contact on request.

EXPERIMENTAL MODEL AND SUBJECT DETAILS

Mosquito rearing

The source and maintenance of the mosquitoes has been described previously (Liu et al., 2020). *Ae. albopictus* were collected from Kaohsiung in 2003. The *Ar. subalbatus* colony was obtain from the National Institute of Preventive Medicine, Taipei, Taiwan, in 1992 and has been kept in our insectary since 2002. *Cx. quinquefasciatus* were collected from Yunling in 2007. The mosquitoes are reared at 26 $\pm$ 1°C and 70-80% relative humidity on a 14 hrs light: 10 hrs dark photoperiod under standard laboratory conditions. All adult mosquitoes are fed with a 10% sugar solution. Female mosquitoes are blood-fed on anesthetized mice once every two weeks. Larvae are fed a mixture of goose liver powder (NTN Fishing Bait LTD., Taiwan) and yeast powder (Taiwan Sugar Corp., Taiwan) (1:1).

Double-stranded RNA synthesis and injection

All dsRNA synthesis was carried out as previously described (Liu et al., 2017). The double-stranded RNA (dsRNA) of the target genes were synthesized using a MEGAscript™ T3/T7 transcription kit (Thermo Scientific, USA). In brief, 1 μg linearized plasmid template was used as template in a 20 μL *in vitro* transcription reaction. The reaction was incubated for 4 hrs at 37°C, followed by adding 1 μL DNase and treating for 15 min. Equal amounts of single-stranded RNA were added together, then annealed by heating at 100°C for 10 min followed by cooling to room temperature overnight. A total of 1 μg of the dsRNA, was dissolved in 0.5 μL DEPC-treated water, and then this was intrathoracically injected into the pupae using a glass injector linked to a glass capillary needle. Control mosquitoes were injected with 0.5 μL DEPC-treated water containing 1 μg GFP dsRNA. All pupae were injected within 0.5 hr after larval-pupal ecdysis, and total RNA from whole mosquitoes was then collected at several different time intervals after dsRNA injection. RT-qPCR was used to detect the effects of dsRNA-based gene silencing on the target genes. The cumulative mortality rates (%) of uninjected control and the dsRNA-injected mosquitoes were compared using one-way ANOVA and Tukey's test ($p < 0.01$).

Ethics approval and consent to participate

Both female and male of mice were 2-3 months old, when used. All mice that were used as a source of blood for mosquitoes were treated in an accordance with the institutional Animal Care and Use Committee

(IACUC) of NCHU, Taiwan. The study protocols were reviewed and approved by the Committee on Animal Research and Care in NCHU (No. 102-76, 23 October 2013 to 17 October 2018). All efforts were made to minimize suffering of the mice.

METHOD DETAILS

Sequence alignment and phylogenetic analysis

The multiple sequence alignment of cecropin from insects, nematodes and tunicates (retrieved at http://www.ncbi.nlm.nih.gov/, http://201.131.57.23:8080/data/triatoma, http://ensemblgenomes.org/, http://acypicyc.cycadsys.org/ and https://hymenoptera.elsiklab.missouri.edu/) were performed using Clustal Omega (https://www.ebi.ac.uk/Tools/msa/clustalo/). The aligned sequences were used to construct Neighbor-Joining phylogenetic trees using MEGA-X. The bootstrap method was used for testing the phylogeny results. The confidence limits of the branch points were estimated using 1,000 bootstrap replications. Amino acid substitution model: p-distance; gaps were treated by pairwise deletion. Numbers at the nodes indicated the bootstrap proportions (only over 50% are showed).

RNA extraction

Twenty whole mosquito bodies were homogenized on ice in 1 mL TRI Reagent® (Merck, USA). After adding 200 μL 1-Bromo-3-chloropropane (Sigma-Aldrich, USA), the mixtures were then incubated on ice for 10 min, which was followed by centrifugation for 15 min at 14,000 g at 4°C. The resultant clear upper aqueous phase was then transferred to a new tube, mixed with an equal volume of ice-cold 2-propanol (Sigma-Aldrich, USA) and incubated on ice for 15 min. This was followed by centrifugation at 14,000 g for 15 min at 4°C. The supernatant was removed, and the RNA pellet was washed twice with 1 mL cold 75% EtOH. The RNA pellet was dried at 65°C for 2 min and then was re-suspended in RNase-free water. The concentration of the RNA samples were then assessed using a NanoDROP™ 2000 spectrophotometer (Thermo Scientific, USA). All RNA samples were stored at −80°C.

Reverse transcription-quantitative PCR (RT-qPCR) analysis

The relative expression of a gene was analyzed by RT-qPCR. RT was performed using a RevertAid™ First Strand cDNA Synthesis Kit (Thermo Scientific, USA) according to the manufacturer's protocol. The specific primer pairs used for the RT-qPCR are shown in Table S1. The sequences of the above PCR products, as amplified by the specific primer pairs, were confirmed by sequencing. All of qPCR reactions were conducted using an ABI StepOnePlus™ detection system (Applied Biosystems, USA) and MicroAmp® Optical 8-Tube Strips (Applied Biosystems, USA). Each reaction tube contained 10 μL of 2x ChamQ Universal SYBR qPCR Master Mix (Vazyme Biotech, China), 2.5 μL of 1.6 μM of each gene-specific primer, and 5 μL of 10x diluted cDNA in the total volume of 20 μL. The thermal cycling conditions were initiated by heating to 95°C for 3 min, followed by 40 cycles of 95°C for 15 s and 56°C for 30 s. The data was obtained using triplicate RT-PCR reactions and these were then analyzed to identify any significant differences ($p < 0.005$, one-way ANOVA by Tukey's test).

Protein synthesis

The four synthetic cecropin B peptides used in this study were synthesized by Genemed Synthesis Inc. (USA). The amino acid sequence of Aacec B peptide used in this study is N-GRLKKLGKKIERAGKRVFN AAQKGLPVAAGIKGLGR-C as previously described (Liu et al., 2017). The Ascec B2 peptide sequence is N-GRLKKLGKKIERAGKRVVNAAQKGLPVAAGIQALGR-C. The Aalcec B peptide sequence is N-GRLKKLGK KIEKAGKRVFNAAQKGLPVAAGVKALGR-C. The Cqcec B1 peptide sequence is N-GRLKKLGKKIEKAGKR VFNAVQKGLPVAAGVQALGR-C. The cecropia moth (*Hyalophora cecropia*) cecropin B (Hccec B) peptide, was used as the controls in RNAi phenotype rescue experiments and DNA pull-down assay, sequence was N-KWKVFKKIEKMGRNIRNGIVKAGPAIAVLGEAKAL-C. The *Ar. subalbatus* cecropin B1 (Ascec B1) peptide, was used to test the specificity of Ascec B2 antibody, sequence is N-GFLKKLGKKVEGVGKRVFKASEKALPV VAGYKAVGK-C.

SDS-polyacrylamide gel electrophoresis (SDS-PAGE) and western blotting

SDS-PAGE and Western blotting were carried out as previously described by Liu et al.'s protocol (2017). Each protein sample was mixed with sample buffer containing SDS, DTT and 5% β-mercaptoethanol (β-ME) and then boiled at 100°C for 10 min; then each sample was separated by 10% SDS-PAGE (Toolsbiotech, Taiwan) under reducing conditions. Next the proteins were transferred to a polyvinylidene difluoride

membrane (Millipore, USA) using a transfer apparatus. Anti-β-actin antibody (Santa Cruz Biotechnology Inc., USA), secondary anti-mouse immunoglobulin-horseradish peroxidase (PerkinElmer, Inc., USA), anti-histone H2B antibody (Cell Signaling Technology, USA) and secondary anti-rabbit immunoglobulin-horse-radish peroxidase (KPL, USA) were used for the Western blot analysis. For the production of anti-Ascec B2 antibody, the most variable regions of the peptide sequence across the five Ascecs and *Ae. aegypti* cecro-pin B (Aacec B) were identified by BLAST and antigen prediction. Specifically, the peptide sequence region near the C-terminal end (amino acid sequence N-VNAAQKGLPVAAGIQALGR-C) was identified and used to generate an appropriate antigenic peptide, which was then used for rabbit polyclonal anti-Ascec B2 anti-body generation by Yao-Hong Biotechnology Inc. (Taiwan).

Transmission electron microscopy (TEM)

Sample preparation for TEM was carried out as described by Liu et al.'s protocol (2017). In brief, at least five surviving pupae were randomly selected at 48 hrs (*Ae. albopictus* and *Cx. quinquefasciatus*) or at 72 hrs (*Ar. subalbatus*) after injection and dissected in cold PBS. The third and fourth abdominal fragments were excised and fixed with 3% glutaraldehyde (Electron Microscopy Science, USA) in cacodylate buffer (0.1 M, pH 7.4) (Merck, USA) for 3 hrs at 4°C and then post-fixed in 1% osmium tetroxide in cacodylate buffer (0.1 M, pH 7.4) for 6 hrs at 4°C. After washing three times in cold PBS for 10 min each, the fixed specimens were dehydrated in increasing ethanol concentrations and then embedded in Epon 812 resin (Electron Mi-croscopy Science, USA). The blocks were sectioned using an ultramicrotome (Ultracut; Leica Microsystems, Germany). The ultrathin sections were placed on formvar-coated copper grids (SPI Supplies, Inc., USA), post-stained with 2% uranyl acetate (Merck, USA) and 1% lead citrate (Electron Microscopy Science, USA), and then visualized/photographed using a 100-kV transmission electron microscope (JEOL 2000EX II) (Japanese Electron Optic Laboratory, Japan).

Standard and quantitative chromatin immunoprecipitation (standard ChIP and qChIP)

The standard ChIP assays were carried out as previously described (Liu et al., 2017). Briefly, pupae were homog-enized in PBS (150 mM NaCl, 1 mM CaCl$_2$, 2 mM KCl, and 1 mM NaHCO$_3$, pH 7.0) on ice and any DNA-protein complexes present were cross-linked by the addition of 1% formaldehyde (Sigma-Aldrich, USA) to the samples. The samples were incubated at 37°C for 10 min, and the reaction was then stopped by the addition of glycine (Sigma-Aldrich, USA) to a final concentration of 125 mM at room temperature for 5 min. The ChIP assay was per-formed using a Pierce™ Magnetic ChIP Kit (Thermo Scientific, USA) according to the manufacturer's instructions. Three biological replicates were carried out for the qChIP assay and the amount of precipitated DNA was quan-tified using quantitative polymerase chain reaction as the percentage precipitated relative to each input sample. The primers used in the ChIP and qChIP assays are listed in Table S1.

DNA pull-down assay

The DNA pull-down assay was carried out as previously described (Liu et al., 2017). Synthetic cecropin B peptide (cec B) was covalently crosslinked with TANBead USPIO-101 (Taiwan Advanced Nanotech Inc., Taiwan) through a 1-ethyl-3-(3-dimethylaminopropyl) carbodiimide hydrochloride (Sigma-Aldrich, USA) by coupling reaction in the coupling buffer (100 mM 2-(N-morpholino)-ethanesulfonic acid, 150 mM So-dium chloride, pH 6.0) and then stored at 4°C until use. The cec B peptide-conjugated magnetic beads were incubated with each PPO 3 DNA fragment for 30 min at 25°C under gentle rotation. The bead-cec B peptide-DNA fragment complexes were then collected with a magnet and was washed three times with 1✕ cold PBS containing 0.1% Tween-20, followed by two times with 1x cold PBS. Each bead-cec B pep-tide-DNA fragment complex fraction was then collected again with a magnet and suspended in 50 μL distilled water for subsequent qPCR analysis. The specific primer pairs used to detect the PPO 3 DNA frag-ments are shown in Table S1.

QUANTIFICATION AND STATISTICAL ANALYSIS

GraphPad Prism and Microsoft Excel software were used for statistical analysis. Unless otherwise indicated, a one-way ANOVA by Tukey's test was used to determine differences between treatments. All experiments were performed in triplicate. All data were considered statistically significant at $p < 0.005$ for qPCR or $p < 0.01$ for cumulative mortality rates, and the results are presented as means $\pm$ SD. Statistical details of experiments can be found in the figure legends, figures, and results. *$p < 0.005$; **$p < 0.001$.